

## Dynamics of Complex Phthalate Liquids. 2. Structural Effects of Side Chains

Yoo Joong Kim and Jiri Jonas\*

Department of Chemistry, School of Chemical Sciences and Beckman Institute for Advanced Science and Technology, University of Illinois Urbana, Illinois 61801

Received: December 1, 1997; In Final Form: February 17, 1998

In this paper, the second of a series of two presenting the structural effects on the dynamic properties of complex liquids, we discuss the effect of structural changes in the alkyl side chain on the macroscopic viscosity and microscopic motional behavior of phthalates.  $^{13}\text{C}$  NMR spin–lattice relaxation times and nuclear Overhauser enhancements of individual carbon nuclei of di-*n*-octyl phthalate (DNOP), di-*n*-hexyl phthalate (DHP), and bis(6-methylheptyl) phthalate (DIOP) have been measured as a function of temperature from  $-40$  to  $70$  °C. Individual  $^{13}\text{C}$  peaks were unambiguously assigned by using 2D  $^1\text{H}$ – $^{13}\text{C}$  chemical shift correlation and specific relaxation of individual carbons in the alkyl chain of the molecule. In addition, the density and viscosity of these compounds as a function of temperature have been measured. The results were also compared with earlier experiments performed on bis(2-ethylhexyl) phthalate (DEHP). The optimized parameters of the Cole–Davidson distribution model obtained from the analysis of the  $^{13}\text{C}$  relaxation data provided the detailed information on the internal motions of the alkyl side chains. The NMR relaxation data and shear viscosity of the phthalate liquids were interpreted phenomenologically in terms of the alkyl side chain flexibility. The branching in the alkyl chain restricted the motional degree of freedom of the side chain, which made the molecule less flexible as a whole. The branching near the rigid part of the molecule was found to be more effective in restricting the internal motion of the alkyl chain.

### Introduction

In the preceding paper,<sup>1</sup> hereafter referred to as I, the effect of the structural changes in the molecular framework of phthalates on their dynamic behavior has been investigated. In this paper, we discuss the effect of structural changes in the alkyl side chain of phthalate esters. As pointed out in I, the importance of understanding the structure–property relationships has motivated this systematic study of the effects of structural modifications on dynamic properties in the model lubricant system of complex phthalates, which are composed of relatively rigid framework and flexible side chains. Since the variation of chain length and the presence of the branching in the alkyl chain considerably influence physicochemical properties of functional fluids, it is important to understand in detail the effect of structural variation in the side chain on the macroscopic and microscopic motional behavior.

For this purpose, several liquid phthalates with different side chains have been selected: di-*n*-octyl phthalate (DNOP), diisooctyl phthalate (DIOP),<sup>2</sup> and di-*n*-hexyl phthalate (DHP). As in I,  $^{13}\text{C}$  NMR relaxation data for individual carbon nuclei in these compounds, as well as their density and viscosity, have been measured as a function of temperature from  $-40$  to  $70$  °C. The  $^{13}\text{C}$  NMR relaxation data have been analyzed in terms of the Cole–Davidson distribution model. The information of motional behavior of these compounds are also compared with those of bis(2-ethylhexyl) phthalate (DEHP),<sup>1,3</sup> which represents the model lubricant liquid. A comparison of the motional behavior of three isomers, DIOP, DEHP, and DNOP, provides information as to the influence of branching on the physical properties of these liquids. By comparing DNOP and DHP,

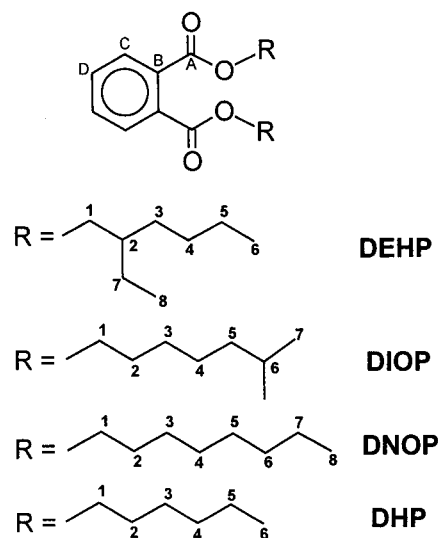


**Figure 1.** Structural formulas of the compounds studied. Carbon atoms are labeled considering chemical equivalence.

the effect of varying the chain length can be examined. The structural formulas of these compounds are shown in Figure 1.

### Experimental Section

The DNOP (98%) and DHP (98%) samples were purchased from Chem Service and used without further purification. All of the commercially available samples of “diisooctyl phthalate” were mixtures of various C-8 isomers, which were unsuitable for the  $^{13}\text{C}$  NMR relaxation study. DIOP (bis(6-methylheptyl) phthalate) was synthesized by esterification of phthalic anhydride with 6-methyl-1-heptanol with phosphotungstic acid ( $\text{H}_3\text{P}$

\* E-Mail: j-jonas@beckman.uiuc.edu. Fax: (217) 244-3993.

**TABLE 1: Carbon-13 Chemical Shift Assignments for the Phthalate Liquids Studied (Chemical Shifts (ppm) Are Relative to TMS)**

carbon <sup>a</sup>	DEHP <sup>b</sup>	DIOP	DNOP	DHP
A	167.0	167.0	166.9	167.1
B	133.0	133.0	132.8	132.9
C	129.0	129.1	128.9	129.0
D	130.9	131.0	130.8	131.0
1	67.6	65.5	65.4	65.5
2	39.1	29.0	28.8	28.8
3	30.7	26.6	26.2	26.0
4	29.2	27.5	29.52	31.8
5	23.2	39.3	29.49	22.8
6	14.2	28.2	32.1	14.1
7	24.0	22.9	22.8	
8	11.1		14.1	

<sup>a</sup> See Figure 1 for the carbon nuclei labels. <sup>b</sup> From I.

PO<sub>4</sub>·12WO<sub>3</sub>·xH<sub>2</sub>O, Aldrich) as a catalyst.<sup>4</sup> 6-Methyl-1-heptanol was also prepared according to the literature<sup>5</sup> using hydroboration of 6-methyl-1-heptene (Wiley Organics). The purity of the final DIOP product was determined by gas chromatography to be 97%.

The experimental details, including density measurements, viscosity measurements, two-dimensional <sup>1</sup>H–<sup>13</sup>C correlation (HETCOR) experiments for <sup>13</sup>C NMR peak assignments, and <sup>13</sup>C NMR relaxation measurements are the same as described in I.

## Results and Discussion

(A) <sup>13</sup>C Peak Assignments. All carbon-13 nuclei of DIOP, DNOP, and DHP were resolved in the <sup>13</sup>C NMR spectra well enough for the relaxation measurements under the experimental conditions, except for carbon nuclei 4 and 5 of DNOP. The two <sup>13</sup>C resonance signals in DNOP have very similar chemical shifts and could not be resolved completely for the relaxation measurements, even in the high magnetic field of 9.3 T.

Using both the <sup>1</sup>H–<sup>13</sup>C chemical shift correlation from the 2D HETCOR spectra and the spin–lattice relaxation time comparison, all of the carbon-13 spectral peaks could be

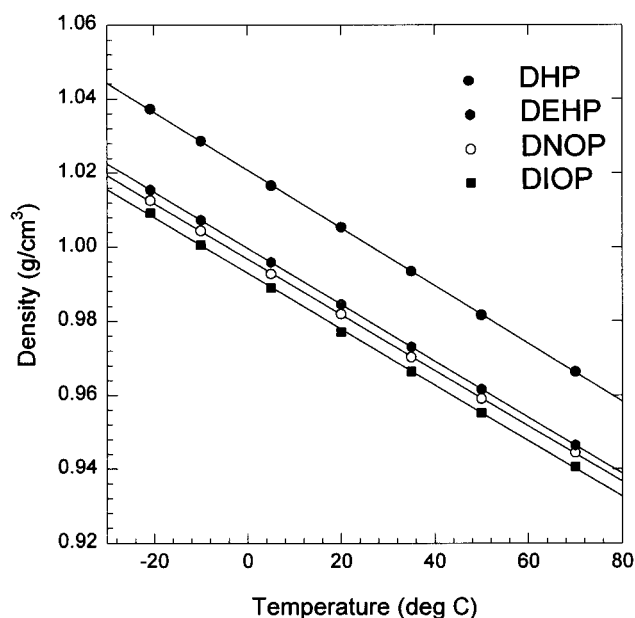


**Figure 2.** Densities of the phthalate liquids studied as a function of temperature.

unambiguously assigned. Taking advantage of the tendency for  $T_1$  values to increase in the motional narrowing regime as one moves away from the ring system along a flexible side chain, the alkyl chain <sup>13</sup>C peaks that have similar chemical shifts were clearly identified.

The <sup>13</sup>C chemical shift assignments, relative to tetramethylsilane (TMS), are listed in Table 1 for all of the compounds studied, including DEHP.<sup>3</sup> The chemical shifts for the carbonyl and the phenyl ring carbons (A–D), which are the common structural framework in these molecules, are practically the same for all of the phthalates.

(B) Density and Viscosity Measurements. The temperature dependencies of the density for the compounds studied are shown in Figure 2. The density for each of these liquids are very well represented as a linear function of temperature, and

**TABLE 2: Temperature Dependence of <sup>13</sup>C Spin–Lattice Relaxation Times (seconds) for the Proton-Bearing Carbon Nuclei of DIOP Measured at 100.6 MHz**

carbon	66.2 °C	51.4 °C	38.5 °C	29.5 °C	19.9 °C	6.7 °C	–3.8 °C	–15.1 °C	–26.5 °C	–36.2 °C
C	0.412	0.300	0.239	0.208	0.192	0.207	0.272	0.466	0.903	
D	0.384	0.277	0.220	0.191	0.178	0.200	0.277	0.535	1.06	
1	0.522	0.362	0.271	0.229	0.200	0.188	0.194	0.220	0.273	0.374
2	0.670	0.462	0.351	0.287	0.240	0.200	0.189	0.192	0.234	0.306
3	0.878	0.602	0.438	0.362	0.297	0.239	0.210	0.208	0.225	0.269
4	1.09	0.740	0.555	0.444	0.364	0.289	0.253	0.242	0.243	0.302
5	1.31	0.972	0.688	0.550	0.438	0.331	0.279	0.251	0.248	0.255
6	2.85	1.98	1.46	1.12	0.838	0.634	0.516	0.457	0.448	
7	2.52	1.89	1.49	1.19	0.891	0.629	0.479	0.347	0.267	0.212

**TABLE 3: Temperature Dependence of <sup>13</sup>C Spin–Lattice Relaxation Times (seconds) for the Proton-Bearing Carbon Nuclei of DNOP Measured at 100.6 MHz**

carbon	66.2 °C	51.4 °C	38.5 °C	29.5 °C	19.9 °C	6.7 °C	–3.8 °C	–15.1 °C	–26.5 °C	–36.2 °C
C	0.456	0.331	0.259	0.220	0.196	0.194	0.230	0.349	0.601	1.10
D	0.407	0.294	0.235	0.202	0.180	0.190	0.230	0.373	0.699	1.30
1	0.560	0.390	0.294	0.247	0.208	0.187	0.188	0.203	0.239	0.302
2	0.700	0.507	0.380	0.310	0.252	0.208	0.189	0.184	0.201	0.240
3	0.946	0.659	0.496	0.396	0.321	0.257	0.223	0.207	0.206	0.223
4/5 <sup>a</sup>	1.24	0.890	0.659	0.532	0.435	0.340	0.286	0.257	0.246	0.252
6	2.01	1.41	1.03	0.808	0.632	0.482	0.392	0.331	0.297	0.284
7	2.90	1.90	1.47	1.15	0.898	0.641	0.501	0.397	0.342	0.311
8	4.99	3.89	2.83	2.35	1.88	1.38	1.07	0.832	0.649	0.520

<sup>a</sup> The peaks for carbons 4 and 5 overlap due to similar chemical shifts. The  $T_1$ 's reported here are the values for the overlapping peaks which may be considered as an average of the  $T_1$ 's for carbons 4 and 5.

**TABLE 4: Temperature Dependence of  $^{13}\text{C}$  Spin–Lattice Relaxation Times (seconds) for the Proton-Bearing Carbon Nuclei of DNOP Measured at 45.2 MHz**

carbon	68.7 °C	49.8 °C	30.8 °C	20.0 °C	9.1 °C	−0.6 °C	−14.0 °C	−23.6 °C	−32.8 °C	−42.7 °C
C	0.480	0.281	0.160	0.131	0.106	0.101	0.127	0.171	0.304	
D	0.458	0.259	0.148	0.119	0.103	0.0993	0.131	0.180	0.316	
1	0.518	0.303	0.172	0.135	0.107	0.0895	0.0901	0.0943	0.108	0.124
2	0.741	0.428	0.253	0.181	0.133	0.109	0.0897	0.0888	0.0963	
3	0.985	0.567	0.323	0.234	0.170	0.137	0.112	0.0985	0.0978	0.102
4/5 <sup>a</sup>	1.27	0.733	0.419	0.300	0.228	0.182	0.144	0.128	0.125	0.123
6	2.07	1.21	0.679	0.495	0.346	0.272	0.202	0.172	0.159	0.146
7	3.09	1.82	1.03	0.742	0.502	0.378	0.263	0.218	0.187	0.166
8	5.68	3.80	2.33	1.79	1.27	0.961	0.676	0.555	0.462	0.399

<sup>a</sup> The peaks for carbons 4 and 5 overlap due to close chemical shifts. The  $T_1$ 's reported here are the values for the overlapping peaks which may be considered as an average of the  $T_1$ 's for carbons 4 and 5.

**TABLE 5: Temperature Dependence of  $^{13}\text{C}$  Spin–Lattice Relaxation Times (seconds) for the Proton-Bearing Carbon Nuclei of DHP**

carbon	68.4 °C	49.7 °C	30.8 °C	20.0 °C	9.8 °C	−1.3 °C	−12.8 °C	−24.5 °C	−33.0 °C	−43.5 °C
C	0.602	0.365	0.203	0.151	0.119	0.101	0.102	0.146	0.241	
D	0.563	0.325	0.186	0.135	0.109	0.0954	0.105	0.151	0.264	
1	0.719	0.409	0.231	0.169	0.128	0.100	0.0898	0.0905	0.0976	0.122
2	1.10	0.627	0.352	0.258	0.174	0.128	0.0995	0.0892	0.0882	0.100
3	1.62	0.955	0.517	0.359	0.250	0.174	0.135	0.110	0.105	0.112
4	2.27	1.37	0.728	0.520	0.350	0.247	0.186	0.149	0.140	0.139
5	3.27	1.94	1.04	0.724	0.515	0.354	0.253	0.191	0.164	0.158
6	5.43	3.77	2.32	1.78	1.30	0.923	0.693	0.527	0.441	0.359

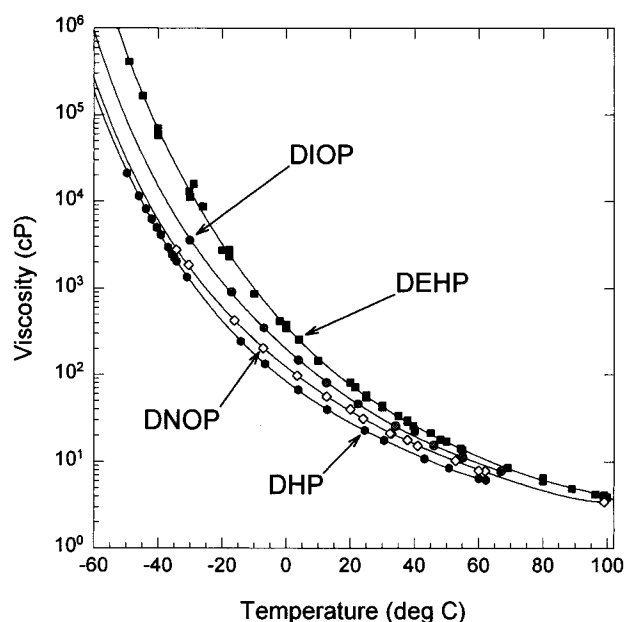


**Figure 3.** Viscosities of the phthalate liquids studied as a function of temperature. Data for DEHP was copied from I. DNOP solidified at  $-35$  °C.

the temperature–density coefficients of these liquids are nearly the same ( $(7.6 \pm 0.2) \times 10^{-4} \text{ g/cm}^3 \cdot \text{°C}$ ).

The viscosities of the phthalate liquids as a function of temperature are shown in Figure 3, where the temperature–viscosity dependencies of each of the phthalate liquids are well described by the Vogel–Fulcher–Tammann (VFT) equation<sup>6</sup> over the experimental temperature range. By comparing the viscosity of the three C-8 phthalate isomers, it is obvious that the presence of a branch in the alkyl chain makes the fluid more viscous. The branch also seems to be more effective in increasing viscosity if it is located near the rigid ring part of the molecule (DEHP > DIOP).

Besides viscosity, the temperature coefficient of viscosity is another important bulk property in determining the performance characteristics of functional fluids including lubricants.<sup>7</sup> The

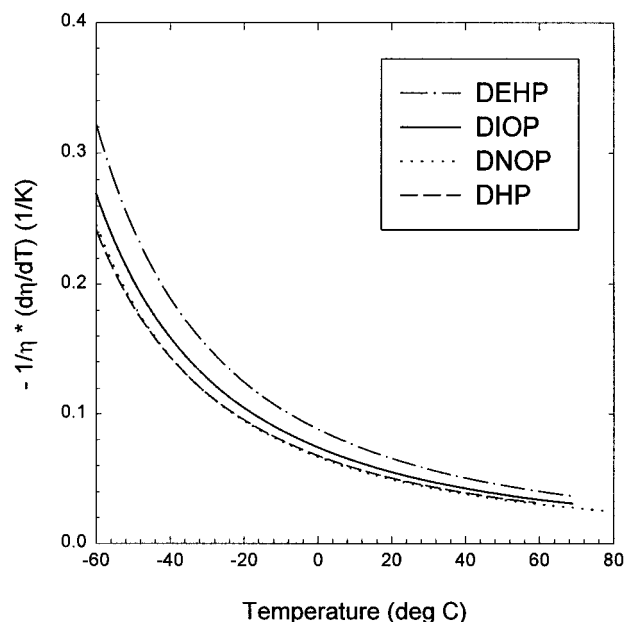


**Figure 4.** Temperature coefficient of viscosity,  $-(1/\eta)(d\eta/dT)$ , of the phthalate liquids studied. The curves were obtained by numerical differentiation of the analytical function of the VFT form fitted by the experimental viscosity data.

smallest possible temperature coefficient of viscosity (or lowest viscosity–temperature slope) is usually desirable for a wide working range of temperature. The temperature coefficients of viscosity ( $-(1/\eta)(d\eta/dT)$ ) of the phthalate liquids are shown in Figure 4. The curves in the figure were obtained by fitting the experimental viscosity data to generate an analytical function of VFT form and then numerically differentiating the resultant function.<sup>8</sup> Interestingly, two phthalates with unbranched side chains, DNOP and DHP, have very similar temperature coefficients of viscosity, although the absolute magnitude of viscosity of DNOP is larger (in Figure 3) owing to its greater molecular weight. Considering that the temperature coefficient of viscosity depends on the molecular flexibility,<sup>9</sup> this result suggests that the alkyl side chains of DNOP and DHP have a

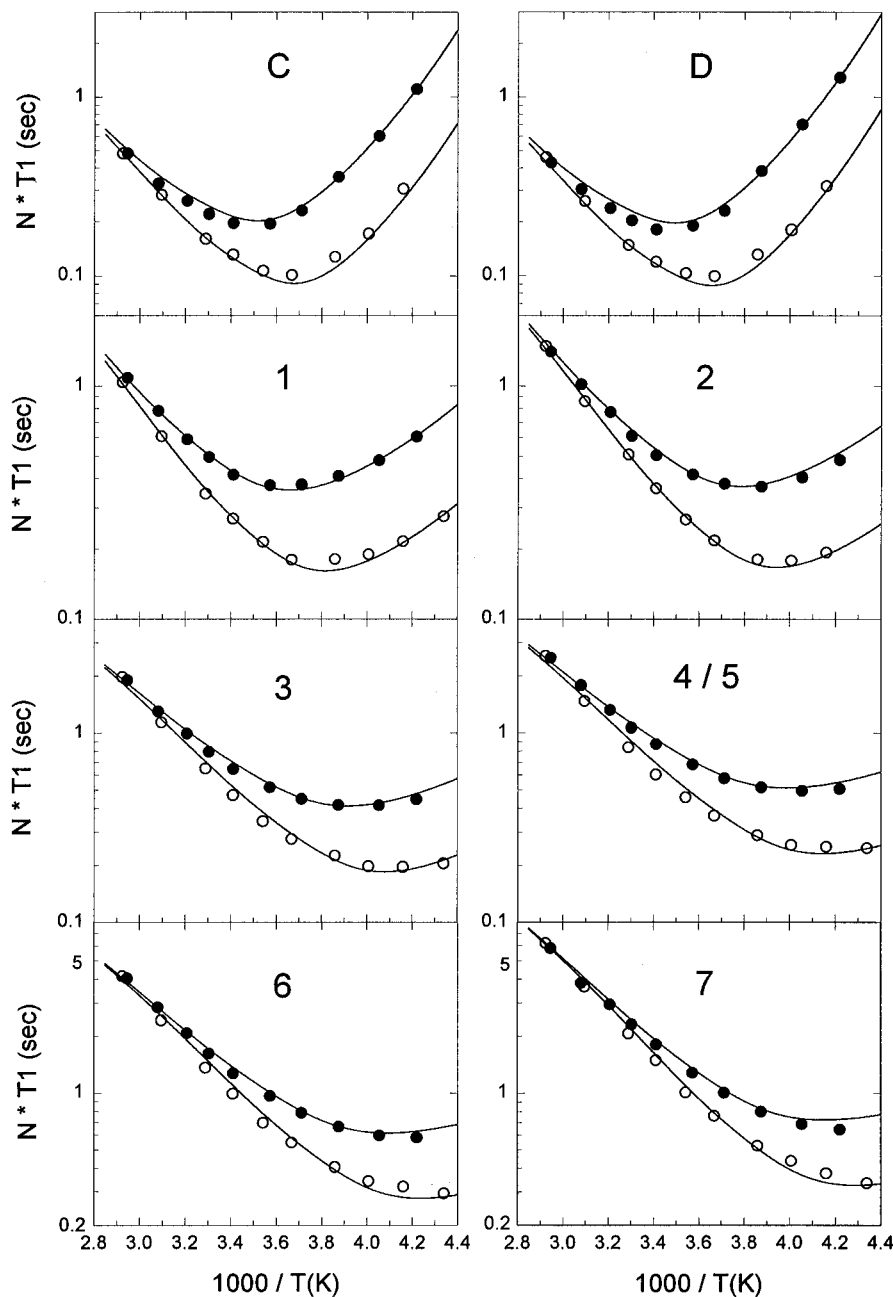


**Figure 5.**  $^{13}\text{C}$   $N \cdot T_1$ 's of DNOP fitted by the Cole–Davidson distribution model. Solid circles indicate the experimental  $T_1$ 's at 100.6 MHz and open circles at 45.2 MHz. The lines represent the fitting results using the optimized parameters.

similar degree of flexibility. The temperature coefficients of the phthalate esters with branched side chains are higher than those with unbranched side chains, which is also understandable because the branching reduces the flexibility of the alkyl chain by restricting internal rotation of the chain. The flexibility of the alkyl side chain seems to be reduced more by branching near the rigid ring/carboxyl group (in DEHP) than by branching near the end of chain (in DIOP).

**(C)  $^{13}\text{C}$  NMR Relaxation Data Analysis.** The low-temperature limit of the spin–lattice relaxation times ( $T_1$ ) and nuclear Overhauser enhancement (NOE) measurements for individual  $^{13}\text{C}$  nuclei was again determined by a low signal-to-noise ratio or inability to resolve the individual peak at that temperature. The experimental  $T_1$  data as a function of temperature are presented in Tables 2–5 for proton-bearing carbon nuclei in DIOP (measured at 100.6 MHz), DNOP (both at 100.6 and 45.2 MHz), and DHP (45.2 MHz). Two  $^{13}\text{C}$  peaks with similar intensity for carbons 4 and 5 in DNOP were not resolved well

as mentioned above, and the  $T_1$ 's reported here are the data for the overlapping peaks. These  $T_1$  values were assumed to be the average of the  $T_1$ 's for the two  $^{13}\text{C}$  nuclei.

The experimental relaxation data for the individual carbon nuclei, except for the methyl carbons, were analyzed in terms of a model assuming a Cole–Davidson distribution of relaxation times. The inadequacy of the analytical methods for the quaternary (A and B) and methyl carbons has been discussed in the earlier papers.<sup>1,3</sup> For the relationship between temperature and correlation time, the limiting correlation time  $\tau_0$  in the Cole–Davidson distribution model was assumed to have a VFT temperature dependence, and  $T_0$  for each compound was determined by fitting the temperature-dependent viscosity data in Figure 3 as in I. The experimental relaxation data for DIOP, DNOP, and DHP were very well represented by the Cole–Davidson distribution model. The optimized set of parameters of the model simultaneously represented the experimental  $T_1$  and NOE data at a single frequency, as well as the  $T_1$  data at

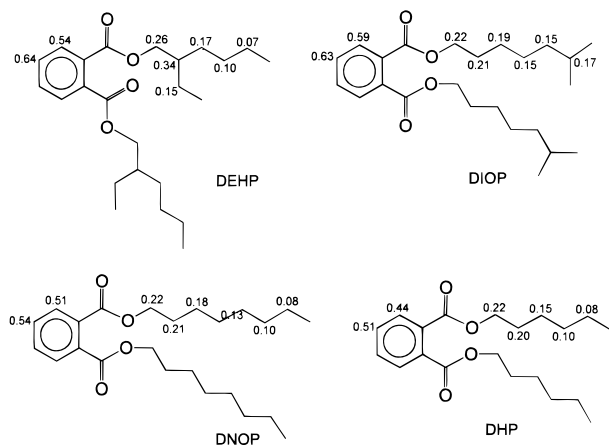


**Figure 6.** Comparison of the  $\beta$  values in the Cole–Davidson distribution model for the analyzed carbon nuclei in the phthalates studied. The  $\beta$  values for DEHP are from I.

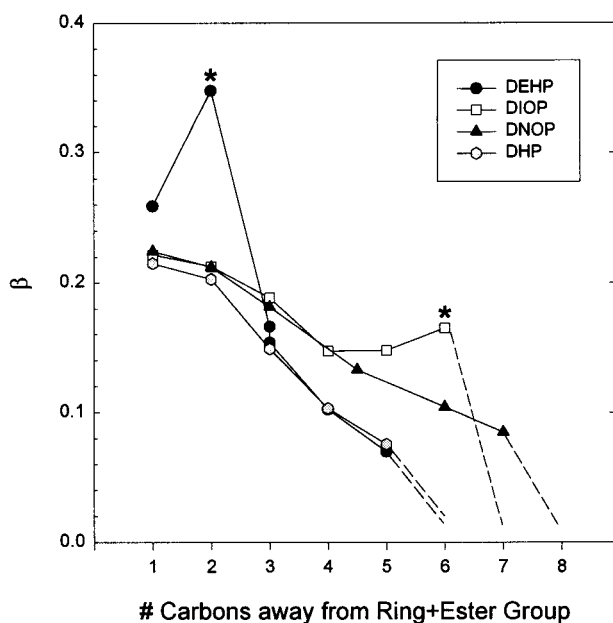


**Figure 7.**  $\beta$  values of the side chain carbons versus the distance from the rigid framework (the phenyl ring and carboxyl group) in units of carbon atoms.  $\beta$  values for the methyl carbons are indicated as dotted lines only for the purpose of avoiding confusion in locating the end of the alkyl chains. Asterisks indicate the branching point, which is carbon 2 in DEHP and carbon 6 in DIOP.

two different frequencies as in the case of DNOP. As an illustration, the resultant fits of  $N \cdot T_1$ 's as a function of temperature for the individual  $^{13}\text{C}$  nuclei in DNOP using the Cole–Davidson distribution model are shown in Figure 5.

Interpretation of the optimized parameters of the Cole–Davidson distribution model provides useful information on the motional behavior of these molecules. Among the parameters, the distribution width,  $\beta$ , contains information on the detailed motional features of each carbon atom of the molecule. The optimized values of  $\beta$  for the individual carbon nuclei of the compounds are shown in Figure 6. In all of the molecules, the  $\beta$  value for carbon D is higher than that of carbon C, indicating the prevailing reorientation along the axis perpendicular to the D–D' bond.<sup>3</sup>

The main points of interest in this investigation are the  $\beta$  values for the alkyl carbons in the side chains of the molecules. The  $\beta$  values of the side chain carbons are plotted in Figure 7, where the  $x$ -axis is the distance from the relatively rigid

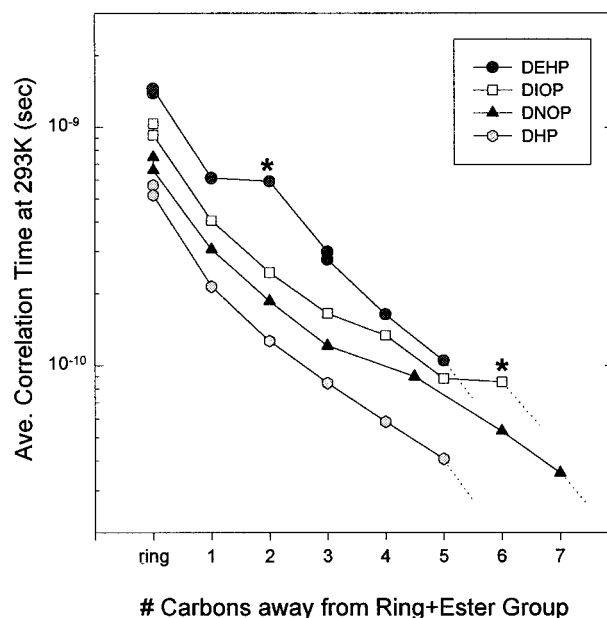


**Figure 8.** Average correlation times ( $\bar{\tau} = \beta\tau_0$ ) for the alkyl carbons of the phthalate liquids studied. Asterisks indicate the branching point, which is carbon 2 in DEHP and carbon 6 in DIOP.

framework (the phenyl ring and carboxyl group) in units of carbon atoms. In this figure,  $\beta$  values for the methyl carbons, which are very low ( $\leq 0.02$ ) and physically meaningless, are indicated as a dotted line only for the purpose of avoiding confusion in locating the end of the alkyl chain. The  $\beta$  values of alkyl carbons generally decrease as one moves away from the relatively rigid part of the molecule to the end of the chain, indicating mobility gradients along the alkyl chain. Comparing the mobility gradients of DNOP and DHP, both of which have unbranched side chains with different lengths, the total decreases of the  $\beta$  values along each alkyl chain are nearly the same (from 0.22 for C-1 to 0.08 for C-( $n - 1$ )) due to the steeper gradient of the shorter chain of DHP. That is,  $^{13}\text{C}$  nuclei in both chains take a similar range of  $\beta$  values. This result implies that the flexibilities of both side chains are similar, which can be related to the similar temperature coefficients of viscosity of these two compounds in the previous section (Figure 4).

The most conspicuous feature in Figure 7 is that the  $\beta$  value of the carbon atom at the branching point (carbon 2 in DEHP and carbon 6 in DIOP, which are indicated in the figure) is large compared to those of the other alkyl carbons. Also the  $\beta$  value for the carbon atom “before” the branching point (carbon 1 in DEHP and carbon 5 in DIOP) appears to have increased. The higher  $\beta$  value in the Cole–Davidson distribution model indicates a narrower distribution of correlation times in the spectral density function, which implies in this case that the number of modes of internal motion is smaller. In other words, the internal motion of an alkyl chain is restricted by the presence of the branch, especially at the branching point. The branching also seems to affect the motional freedom of the C–H internuclear vector adjacent to the branching point, especially nearer to the relatively rigid part of the molecule. Obviously a restriction of the internal motion reduces the flexibility of the alkyl chain, and macroscopically results in enhanced viscosity and temperature coefficients (Figures 3 and 4).

Comparing the rise in the  $\beta$  value at the branching point in DEHP with that in DIOP, the position of branching seems to be also important, and the extent of motional restriction appears to be affected by the proximity of the branching point to the relatively rigid framework of phthalate. In fact, the larger  $\beta$

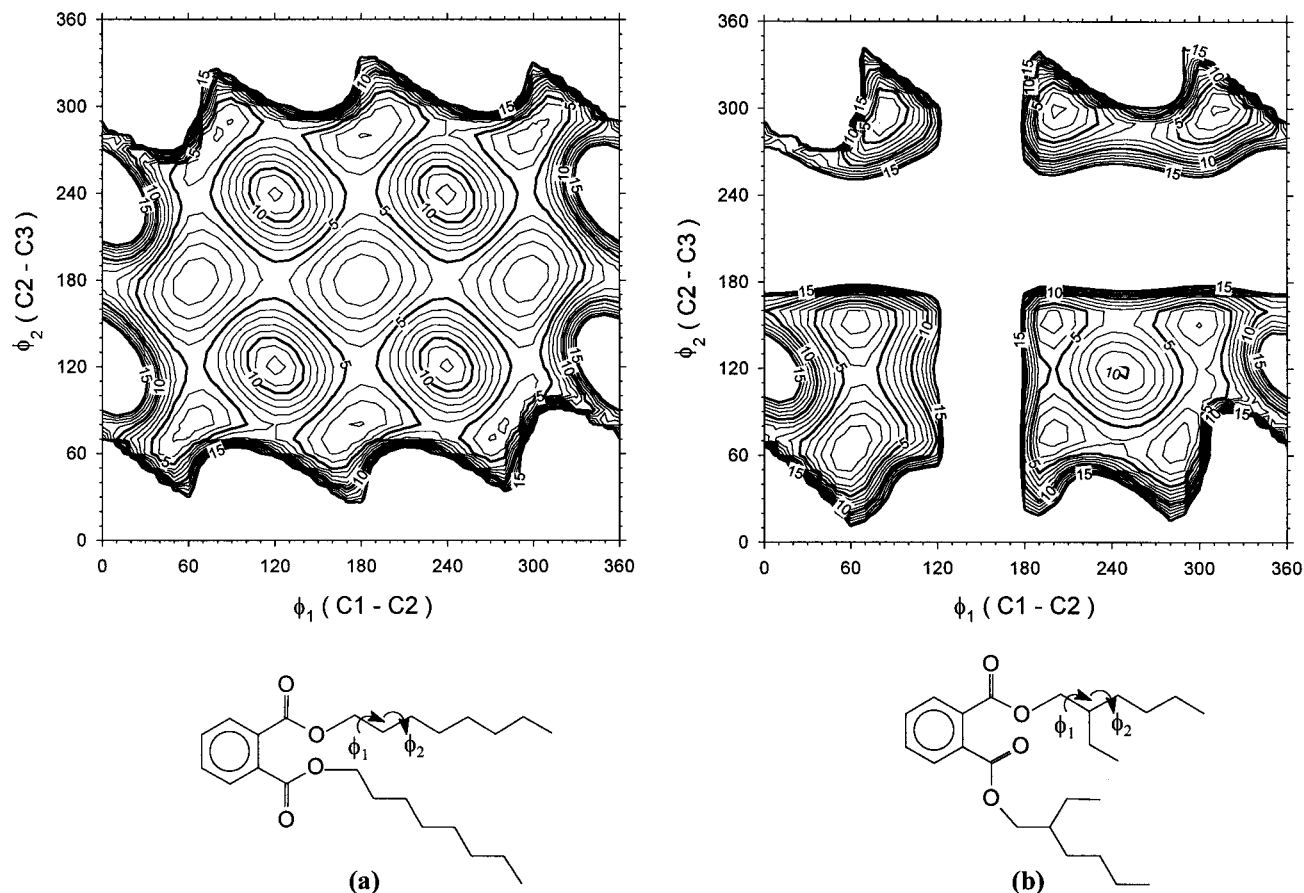


**Figure 9.** Energy contour plot of the conformational space composed of  $\phi_1$ – $\phi_2$  (a) for an unbranched alkyl chain in DNOP and (b) for a branched chain in DEHP. The figures on the contour represent strain energy in kcal/mol relative to the global minimum in the conformational space. The contours up to 15 kcal/mol above the minimum are shown here, beyond which the conformation is considered to be inaccessible.

value at the branching point does not necessarily mean that the correlation time for the C–H internuclear vector at the branching point is greater than that of the other carbons. The average correlation times ( $\bar{\tau} = \beta\tau_0$ ) for the alkyl carbons are plotted in Figure 8. The limiting correlation time ( $\tau_0$ ), which represents the slowest process (or overall motion) of the molecular motion, decreases along the alkyl side chain away from the rigid framework. As the distance from the rigid part of the molecule increases, the effect of the overall motion of the ring at the site of the side chain carbon diminishes more effectively due to the extensive segmental motion of the alkyl chain. This is also accompanied by an increase in motional freedom indicated by a decrease in the  $\beta$  values (mobility gradient). In a branched side chain, the internal motion of the alkyl chain is restricted at (or near) the branching point. If the branching point is far from the phenyl ring, however, the effect of the restriction should decrease due to the internal motions of the preceding part of the alkyl chain. In this respect, branching near the rigid ring portion of the molecule would appear to be more effective in reducing the flexibility of the alkyl chain in the molecule, which also agrees with the macroscopic observation that the temperature dependence of viscosity in DEHP is larger than that of DIOP.

The effect of branching on the restriction of the internal motion can be illustrated by examining the conformational space for the flexible alkyl chain. Figure 9 compares the contour of strain energy calculated by the UFF force field<sup>10</sup> in the conformational space composed of two torsional angles,  $\phi_1$  and  $\phi_2$ , around the branching point in DEHP (a) and for an unbranched alkyl chain in DNOP (b). For the branched chain,

the available conformational space is more restricted compared to the unbranched alkyl chain, and the energy wells in the conformational space are steeper implying higher energy barriers to rotation about these torsional angles. Consequently the internal motions of the alkyl chain are restricted by the presence of the branch, which reduces the flexibility of the molecule.

### Conclusion

The effect of structural changes in the side chains of phthalates on their motional characteristics could be investigated by the <sup>13</sup>C NMR relaxation data analyzed in terms of the Cole–Davidson distribution model. The presence of a branch in the alkyl side chain of phthalate liquids was found to restrict the internal motion of the alkyl chain and consequently reduce the flexibility of the molecule, which was also confirmed by using molecular modeling. The branching near the rigid-ring portion of the molecule was more effective in restraining the motional degree of freedom of the alkyl chain in the molecule. The microscopic motional features of the alkyl chain could be related to the macroscopic viscosity and its temperature dependence, which is the most significant bulk property in deciding the performance characteristics of functional fluids including lubricants.

**Acknowledgment.** This work was supported in part by the Air Force Office for Scientific Research under Grant AFOSR F49620-93-1-0241 and the National Science Foundation under Grant NSF CHE 95-26237.

### References and Notes

- (1) Kim, Y. J.; Jonas, J. J. *J. Phys. Chem. A* **1998**, *102*, 2767.

- (2) In fact, the common name "diisooctyl phthalate" is ambiguous. In this context, it indicates bis(6-methylheptyl) phthalate.
- (3) Kim, Y. J.; Jonas, J. *J. Phys. Chem.* **1995**, *99*, 6777.
- (4) Schwegler, M. A.; van Bekkum, H. *Appl. Catal.* **1991**, *74*, 191.
- (5) Markgraf, J. H.; Lusskin, S. I.; McDonald, E. C.; Volpp, B. D. *J. Chem. Ecol.* **1983**, *9*, 211.
- (6) (a) Fulcher, G. S. *J. Am. Ceram. Soc.* **1923**, *8*, 339. (b) Tammann, G.; Hesse, G. *Z. Anorg. Allg. Chem.* **1926**, *156*, 245. (c) Harrison, G. *The Dynamic Properties of Supercooled Liquids*; Academic Press: New York, 1976.
- (7) Briant, J.; Denis, J.; Parc, G. *Rheological Properties of Lubricants*; Éditions Technip: Paris, 1989.
- (8) Koonin, S. E.; Meredith, D. C. *Computational Physics (Fortran Version)*; Addison-Wesley: New York, 1990; Chapter 1.
- (9) Bondi, A. *Physical Properties of Lubricating Oils*; Reinhold: New York, 1951; Chapter 2.
- (10) Rappé, A. K.; Casewit, C. J.; Colwell, K. S.; Goddard, W. A., III.; Skiff, W. M. *J. Am. Chem. Soc.* **1992**, *114*, 10024.